Applied Surface Science 466 (2019) 772–779

Contents lists available at ScienceDirect

Applied Surface Science

journal homepage: www.elsevier.com/locate/apsusc

Full Length Article

Analysis of dynamic decomposition for barium dimethyl-naphthalene-sulfonate on an Al_3Mg (0 0 1) surface from *ab-initio* molecular dynamics

Jun Zhong[a,*], Xin Li[a], Wenze Ouyang[b], Yuan Tian[a]

[a] School of Materials Engineering, North China Institute of Aerospace Engineering, Langfang 065000, China
[b] Key Laboratory of Microgravity, Institute of Mechanics, Chinese Academy of Sciences, Beijing 100190, China

ARTICLE INFO

Keywords:
ab-initio molecular dynamics
Barium dimethyl-naphthalene-sulfonate
The Al_3Mg (0 0 1) surface
Dynamic decomposition
Design-of-experiment

ABSTRACT

One important dynamic decomposition pathway for a surface corrosion-inhibitor: *barium dimethyl- naphthalene-sulfonate*, is investigated on a clean Al_3Mg (0 0 1) binary-alloy surface using *ab-initio* molecular dynamics based upon density functional theory. Each inhibitor molecule is oriented its functional groups of sulfonic-oxygen bases toward the surface, starting at an initial impact velocity. The dynamic decomposition pathway occurs upon molecular collision with the surface, leading to the decomposed fragments that may clearly represent the initial formation stage of additive thin-film on the surface during a plastic substrate deformation. In addition, three important factors: initial impact speed acting on molecule (kinetic effect), substrate temperature (thermal effect) and initial molecular orientation (geometric effect) etc, are employed to analyze their influences on molecular decomposition. An approach of design-of-experiment (DOE) is applied to an analysis of relative importance for each factor and all factor interactions in above, so as to figure out the best way of surface protection. Final DOE analysis indicates that the most significant factor for promoting molecular decomposition on surface is the substrate temperature, i.e., the higher the substrate temperature, the more rapid decomposition of molecule on surface. While initial impact velocity plays a smaller role, and initial molecular orientation performs less importance to molecular decomposition.

1. Introduction

Petroleum sulfonates such as sodium or barium dialkyl-naphthalene-sulfonates etc, can often be regarded as a kind of anionic surfactant which may play an important role in surface protection [1–4]. These organic molecules are believed to initially react with pure and alloy (clean) metal surfaces through their acid functional groups of sulfonic-oxygen bases (S ~ O-bases), to form a thin-film with several molecular layers thick. And then, they are certain to decompose into several pieces on surfaces to contribute a thin-film cap, i.e., their residual molecular chains (e.g., dialkyl-naphthalene tails) adhered on surfaces by means of S ~ O-bases, would serve as inhibitors to prevent surfaces from further oxidation and corrosion [5–8].

However, the favorably dynamic decomposition pathways for such organic acid molecules through their collisions with solid surfaces have drawn minimal attentions in the literature because these kinds of kinetic reactions usually happened rapidly at the initial critical stage during the processing work, and were thus hardly observed in experiments. Even if, a few of experiments on reactions of small simple molecules with clean metal surfaces, e.g., thermal adsorption and decomposition of H_2O, CH_3OH, CH_3COOH and CH_3OCH_3 molecules on a clean Al (1 1 1) surface etc, were still examined [9–12]. For examples, one examination revealed that, at 90 K these molecules may retard surface oxidization; while above 90 K they would decompose into several pieces to adhere on surface [9]. Underhill and Timsit applied the x-ray photoelectron spectroscopy (XPS) to an analysis of decomposition pathways for 1-butanol and propanoic- acid on a clean Al (1 1 1) surface [13]. They found that, at room temperature, acid molecules broke up on the surface, leading to attachments of aliphatic chain fragments with the surface via C atoms on the fragments. Alternatively, alcohol molecules were found to chemisorb on the surface via its functional (OH) group alone; At elevated temperatures, both acid and alcohol molecules would decompose on the surface via their functional groups, and the dissociated fragments may adhere steadily on the surface. Nevertheless, there continues some uncertainties on decomposition pathways for large complex molecules on metal surfaces during this reaction type.

During past two decades, a technique of computer modeling based upon an *ab-initio* methodology: density functional theory (DFT), has been employed to investigate adsorption and decomposition

* Corresponding author.
E-mail address: setting83@hotmail.com (J. Zhong).

https://doi.org/10.1016/j.apsusc.2018.10.083
Received 2 April 2018; Received in revised form 1 October 2018; Accepted 9 October 2018
Available online 13 October 2018
0169-4332/

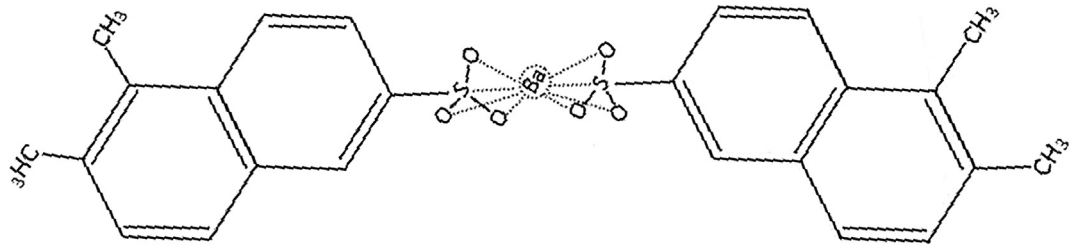

Fig. 1. A schematic of one BDMNS molecular structure.

mechanisms for some molecular additives on metal surfaces. For examples, Jiang and Adams et al calculated adsorption energies of benzotriazole molecules (BTAH, $C_6N_3H_5$) on a clean Cu (1 1 1) surface [14] and a clean Cu_2O (1 1 1) surface [15], respectively. Their calculations indicated that BTAH could be physisorbed or weakly chemisorbed on these surfaces by means of an evolution of its nitrogen sp^2 orbital e^- lone pairs. Following observations of the inelastic electron tunneling spectroscopy (IETS), under the standard state, Hector and Zhong et al investigated reaction enthalpies of vinyl-phosphonic acid (VPA) with an idealized α-Al_2O_3 (0 0 0 1) surface [16] and a clean Al (1 1 1) surface [17], respectively, in three molecular geometries: tri-dentate, bi-dentate, and uni-dentate coordinations. They concluded that the VPA may bond to slab surfaces as a separation consequence of its acid-base: phosphoryl-oxygen (P∼O) and hydroxyl (O-H) groups on surfaces. And, the most favorable adsorption pathway for VPA on surfaces was the tri-dentate geometry, while the uni-dentate one was the least favorable. In addition, computer simulations for boundary thin-film formation on metal surfaces have primarily focused on extremely pressured (kinetic) additives which may minimize wear and corrosion on surfaces when they reacted with some reciprocating surfaces without substrate deformation. For example, a particular additive: zinc dialkyldithio- phosphate (ZDDP) may decompose on iron/steel surfaces to form high strength boundary thin-films [18,19]. By using the Car-Parinello molecular dynamics, Mosey et al. [20,21] predicted that ZDDP boundary thin-films on steel surfaces could be formed solidly by means of a cross-linking of Zn ion with ZDDP main pieces once a certain pressure reached within the thin-film, i.e., if the pressure met the requirement for such the cross-linking reaction, ZDDP may mitigate the surface corrosion. In general, to the best of our knowing, all of above works merely discussed some simple decomposition pathways on clean surfaces. And, despite significant applications of Al-alloys, there were still less modeling works about adsorptions for some particularly large and complex molecules on typically clean Al-alloy surfaces, and even less relevant decomposition pathways on these surfaces.

In this article, we will examine a favorably dynamic decomposition pathway for an important commercial corrosion-inhibitor: barium dimethyl-naphthalene- sulfonate [BDMNS, $Ba(SO_3\text{-}C_9H_5\text{-}2R)_2$, R = a methyl group], on a clean Al_3Mg (0 0 1) surface using *ab-initio* molecular dynamics (AIMD). In this research, each BDMNS molecule was oriented to collide with the clean Al_3Mg (0 0 1) surface through its reactive "oxygen-rich" functional groups (S∼O-bases), so that we can observe whether the decomposed organic acid may adhere on the surface steadily by means of its S∼O-bases or not, and then may prevent metal/alloy surfaces from oxidation or corrosion. Quantities of initial impact velocity acting each molecule toward the surface were extracted from the actual Al-forming work. Bonding characters on each of molecular twigs were depicted in details through the electron localization function (ELF) in the VASP. Simulation results were qualitatively compared with experimental reports using the x-ray photoelectron spectroscopy (XPS) and the electron energy-loss spectroscopy (EELS) for some simple molecules before [9,10], so as to forecast some relevantly decomposing pieces not observed in experiments. To explore an effect of initial molecular orientations on the molecular decomposition, some ancillary calculations were also conducted for each molecule aligned with either its dimethyl-naphthalene- sulfonate rings parallel to the surface or vertical toward the surface. Finally, we analyzed how three factors: the initial impact speed acting on molecule (kinetic effect), the substrate temperature (thermal effect), and the initial molecular orientation (geometric effect), would perform comprehensively during the modeling work. The main goal of this work is to make an understanding: which factor in above would play the significant role in the molecular decomposition.

This article is organized as follows: Section 1 depicts geometries of adsorbate and adsorbent; In Section 2, we present research procedures; In Section 3, we discuss simulation results; In Section 4, we summarize our findings.

2. Conformations of adsorbate and adsorbent

Fig. 1 shows a schematic of a BDMNS structure: one barium (Ba) ion and two dimethyl-naphthalene- sulfonate rings with two respective sulfonic-oxygen bases (S∼O-bases) – the electron-rich functional groups acting as cationic anchors (here, each tail on a ring = one methyl group). Traditionally, according to the Valence Bond Theory [30], one S∼O-base on a pure sulfoacid molecule should appear an "oxygen-rich" tripod with two S═O and one S−O−H groups. However, Fig. 2 shows a side view of the BDMNS backbone structure along with iso-surfaces of charge (e^-) density indicated by the electron (e^-) localization function (ELF) in the VASP, in which a high ELF value means that the reference e^- is highly localized with covalent bonds or inert cores by means of overlaps of e^- clouds [22,23]. Here ELF = 0.86. In this Figure, the bonding status at each of six S∼O bonds looks resonant (quasi-identical), which is very different from that on a pure sulfoacid molecule. The reason was mainly due to a very high ionicity of Ba ion to its neighbors (a bulboid e^- cloud around the Ba ion may just represent this property). As a result, each of two S ions on the BDMNS may evolve its six original valence e^- orbitals to four aniso-sp^3 hybrid ones plus net e^- charges: one sp^3 hybrid orbital was involved in bonding to a dimethyl-naphthalene group, the other three were involved in bonding to three identical O ions (with semilunar lobes) nearby. And then, all of net e^- charges on S and O ions would make these ions link weakly with the Ba ion (the so-called ionic inductivity: no obvious e^- clouds can be seen on these linking bonds, see those dashed lines in Fig. 2). Also in Fig. 2, a spindle e^- cloud on each of Carbon backbone twigs may represent the bonding covalency (σ- or π-type) due to the local hybridization of partial *s* and *p* orbitals on the twig. Since the Ba ion was usually under a free state due to its high ionicity, more net e^- charges of O ions on two S∼O-bases would make these two bases more reactive with metal surfaces than other groups on the BDMNS. According to this character, two dimethyl-naphthalene groups on the BDMNS were assumed not to participate in reacting with metal surfaces during the reactions. Table 1 lists some key bond lengths on the BDMNS as shown in Fig. 2. These data indicated that they were in very good agreements with those in Ref. [17].

Regarding the determination for a specific surface energy, for example, at first, a rectangle slab was constructed with a specific (1 1 1)

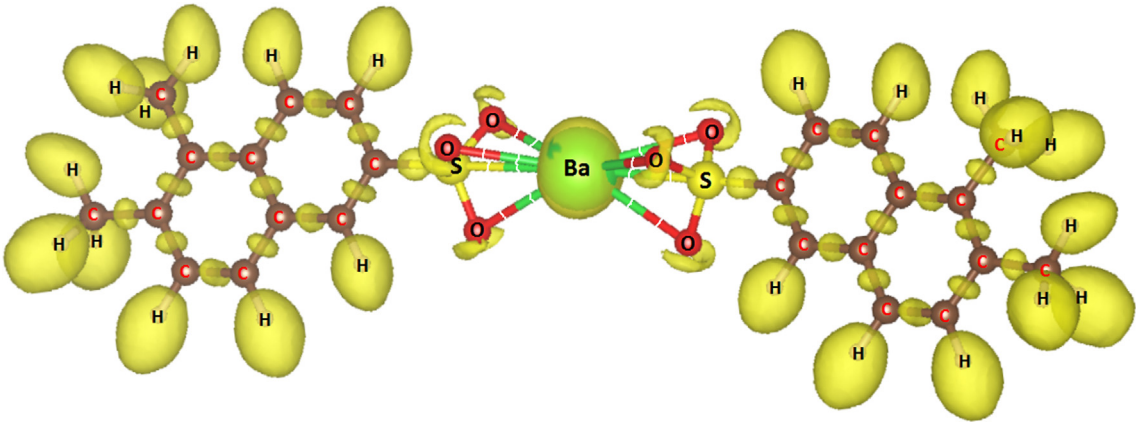

Fig. 2. A side view of one BDMNS backbone structure along with isosurfaces of e^- cloud under ELF = 0.86: black balls: carbon; green balls: barium; red balls: oxygen; yellow balls: sulfur; others: hydrogen.

Table 1
Some important bond lengths on the BDMNS molecule.

Bond type	Bond length	
	Present	Others [14–15,29]
C═C	1.375	1.354–1.378
C−C	1.418	1.392–1.410
C−H	1.090–1.091	1.093–1.094
S ~ O	1.483–1.486	1.422–1.574

surface geometry (a stacking sequence: ABCABC…) normal to the *z*-axis. And then, the total slab energy: E_{slab}, was calculated by the VASP under constraints within a supercell: two periodic boundary conditions along the *x*- and *y*-axes, and a free boundary condition with about 10 Å vacuum spacing along the *z*-axis. Then next, the (1 1 1) surface energy was calculated as follows

$$E_{surf}^{(111)} = \frac{1}{2A_s}(E_{slab} - N \cdot E_{coh}), \quad (1)$$

where A_s was the (1 1 1) surface area of the slab, N the total number of atoms in the slab, and E_{coh} the cohesive energy per ion calculated by the VASP. Please note, the stacking configuration of top layer for each of two slab surfaces must be identical to each other (e.g., a slab with ABCABCA stacking geometry along *z*-direction), so that the calculation for surface energy can be a reasonable output, see ref.[15].

Table 2 lists some relevant surface energies calculated by Eq. (1) for the Al-Mg binary-alloys with different oriented slab substrates. In this Table, the Al_3Mg (1 1 1) surface energy showed the lowest, implying that this surface may be more likely to expose in the air than others. However, under the actual environment, since surface energies of Al_3Mg (1 1 1) and Al_3Mg (0 0 1) slabs were either less than or around a magnitude order of the van der Waals's value (i.e., less than and around 0.10 eV should be regarded as a physisorption quantity), they were believed to likely coexit in actual metal surfaces, and thus could be compatible in the air. Moreover, in a specific slab, for example, if a size of about 17 × 17 × 7 $Å^3$ rectangle was selected, to obey a stoichiometry for Al:Mg = 3:1 in the slab (here Al is the matrix phase, Mg the reinforced phase), the ratio of Al to Mg ions in the Al_3Mg (1 1 1) slab would be 108:36, while that in the Al_3Mg (0 0 1) one was 72:24. Therefore, for an economic reason of material savings in reality, the Al_3Mg (0 0 1) slab would be certainly selected for present research. Fig. 3 shows a top view of the Al_3Mg (0 0 1) surface configuration (cubic type).

Table 2
Some surface energies for Al-Mg binary-alloy substrates (unit: eV/$Å^2$).

Surface type	Surface energy
Al_3Mg (0 0 1) [Cubic]	0.1005
Al_3Mg (1 1 1) [Cubic]	0.0321
Al_2Ti (0 0 1) [BCT]	0.2183

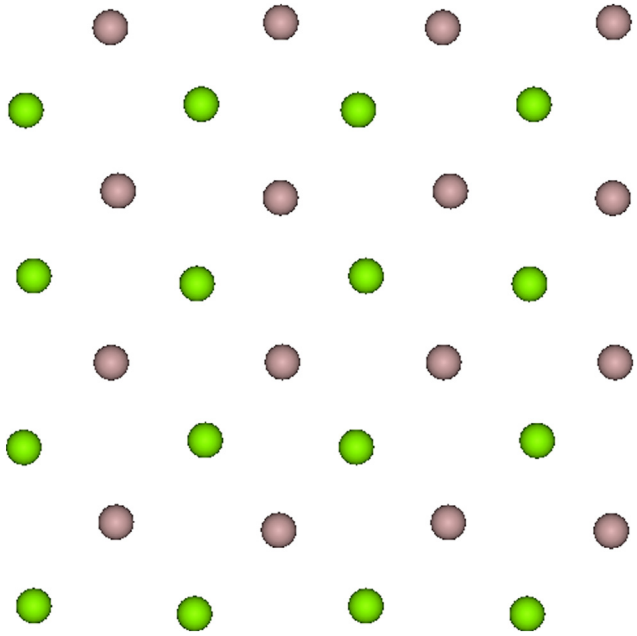

Fig. 3. Top view of the Al_3Mg (0 0 1) cubic slab surface (pink: Al ion, green: Mg ion).

3. Simulation methodologies and procedures

In this research, all of *ab-inito* molecular dynamics (AIMD) simulations based upon density functional theory (DFT) were implemented by the Vienna Simulation Package (VASP) in which pseudo-potentials based upon the projector-augmented wave (PAW) were utilized for elemental constituents [23]. Also, the GGA was considered a reasonable compromise since highly colliding speeds acting on molecules toward slab surfaces would likely overwhelm any barrier to molecular decomposition.

Before all of the AIMD simulations for molecular decomposition on surfaces, at first, the lattice constant (a_0) of a regular Al_3Mg bulk was calculated using the NPT ensemble, which thermally equilibrated one $3a_0 \times 3a_0 \times 3a_0$ unit cell at a temperature of 300 K plus an ambient

pressure of 1.00 bar for about 1500 time steps, a simulation time step = 0.001 picoseconds (ps) [24]. A regular monkhorst-grid of 3 × 3 × 3 was chosen as the best *k*-point sampling for the unit cell [25]. Total energy of this system was converged within 1 ~ 2 meV/atom. A plane-wave cutoff energy: 450 eV, was adopted in all simulations. The computed lattice constant for the Al_3Mg bulk: a_0 = 4.15(8) Å at 300 K, which was in agreement with other calculations and experimental results [26].

Secondly, to simulate interactions between one BDMNS molecule (55 ions) and an Al_3Mg (0 0 1) slab surface, a monkhorst-grid of 3 × 3 × 1 was selected for the best *k*-point sampling [25]. A supercell was constructed with an entire Al_3Mg (0 0 1) slab consisting of three layers (32 ions per layer) of 96 ions. This tetragonal geometry had three definite orientations: $a[1\,0\,0] = 4a_0$ along the x-axis, $b[0\,1\,0] = 4a_0$ along the y-axis, and $c[0\,0\,1] = 40.0$ Å along the z-axis plus a vacuum distance of 20 Å in the *c* direction to preclude interactions with periodic images. The bottom layer of the slab was fixed along the *c* direction to prevent a motion of the slab along this direction when an additive molecule impacted onto the slab surface. In this framework, each of isolated BDMNS molecules was optimized in the same vacuum supercell as used for the Al_3Mg (0 0 1) slab in above. And then, it was equilibrated at 300 K for about 1500 time steps by re-scaling thermal velocities at each time step [27], the time step = 0.001 ps. Simultaneously, the Al_3Mg (0 0 1) slab was equilibrated in its supercell by the same thermal technique as what each of isolated BDMNS molecules did. In the end, each of those isolated BDMNS molecules was transferred into a simulation supercell containing the Al_3Mg (0 0 1) slab, respectively, to build up all relevant reaction systems.

Thirdly, after thermal equilibrations, all of the AIMD simulations for interactions of BDMNS molecules with the Al_3Mg (0 0 1) surface were fulfilled by a constant energy method (NVE) without controlling the system temperature [24]. During the actual processing work, when a painting gun sprayed anti-corrosive liquids toward the Al-alloy surfaces, the highly pressured gradients (kinetics) would draw additive molecules at very high impact speeds toward the surfaces [4,6–8]. Hence, two ultimate approaching speeds acting on the BDMNS molecules, V_z = 1000 and 3000 m/s, were adopted in the AIMD simulations. Then next, each BDMNS molecule started accelerating toward the Al_3Mg (0 0 1) slab surface once it met a net attraction from the surface. To save computational cost, the initial vertical spacing between one BDMNS molecule and the Al_3Mg (0 0 1) surface was set to 2.50 Å, which was slightly larger than the length of Al–O bond (1.86–1.97 Å) as indicated in refs.[17,28]. In addition, for each BDMNS molecule, two initial molecular orientations above the surface were set up: its two dimethyl-naphthalene-sulfonate rings were both vertical (90°) and almost parallel (0°) to the surface, but always with their S ~ O-bases pointing toward the surface, see Fig. 4. These may imitate two ultimate spraying angles from the painting gun in the actual processing work.

Finally, all of systems after the colliding simulations must take the AIMD annealing: two thermal temperatures of 300 K [a_0 = 4.15(8) Å] and 600 K [a_0 = 4.17(7) Å] were chosen as references for the annealing slabs. The purpose of this final work was to analyze which factor in below Section would play the most significant role during molecular decomposition.

4. Results and discussions

4.1. Effects of individual factor

(1). Effect of the initial impact speed: Fig. 5 shows distributions of potential energies for two systems: Mv1 and Mv2, when their BDMNS molecules were colliding vertically towards the Al_3Mg (0 0 1) surface starting at two different initial impact velocities: $\boldsymbol{V}_z = -1000$ and −3000 m/s, and beginning at 300 K for their two slab substrates, respectively. In this Figure, before 50 time steps, these two potential curves looked almost identical because their molecules did not interact with surfaces yet. Around 200 time steps, the Mv2 potential curve appeared a very steep climb because its molecule was reacting with the surface, along with an obvious dissociation: one free Ba ion and two free dimethyl-naphthalene-sulfonate rings from the whole molecule. After 200 time steps, the potential curve oscillated weakly versus the following time steps, meaning that the dissociated pieces bounced off and back the surface to be adsorbing dynamically on the surface via two S ~ O-bases and Ba ion, so as to form stable surface coverings. Also, the substrate temperature rose to about 1100 K from its initial 300 K throughout the whole colliding simulation. As a result, many more Mg ions were segregating into top layer of the surface from the substrate inside, mainly due to a severe change of substrate temperature. This was verified in Refs. [31,32], which may may help prevent the surface from further oxidation, see a graphical Fig. 6(b). However, for the Mv1 system, before 600 time steps, its potential curve was consistently rising slowly, along with a few of small peaks versus the time steps. This meant that the whole BDMNS molecule just showed a tendency of adsorption on the surface but without an obvious dissociation during this time period. After 600 time steps, two dimethyl-naphthalene-sulfonate rings and the Ba ion became obviously dissociating from the whole molecule, and were gradually adsorbing on the surface. And, the substrate temperature rose to about 550 K from its initial 300 K throughout the whole molecular colliding simulation. In this case, it may not lead to Mg ions obvious segregation into top layer of the surface from the substrate inside, see a graphical Fig. 6(a). Also in Fig. 5, an obvious divergence of two potential curves after 200 time steps may represent an apparent change between two substrate temperatures due to low and high speed impacts. Thus, it may conclude that a very high initial

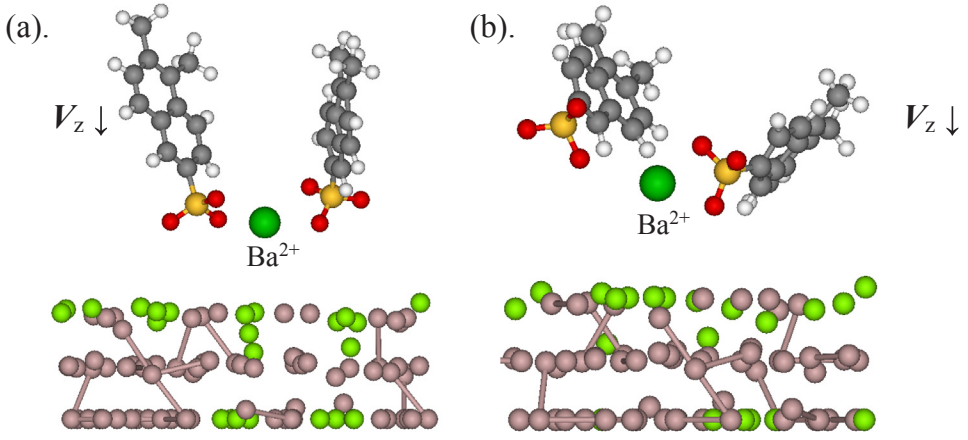

Fig. 4. Side view of a BDMNS collision toward the Al_3Mg (0 0 1) slab surface starting at an impact velocity $\boldsymbol{V}_z$: (a). Vertical geometry; (b). Parallel geometry.

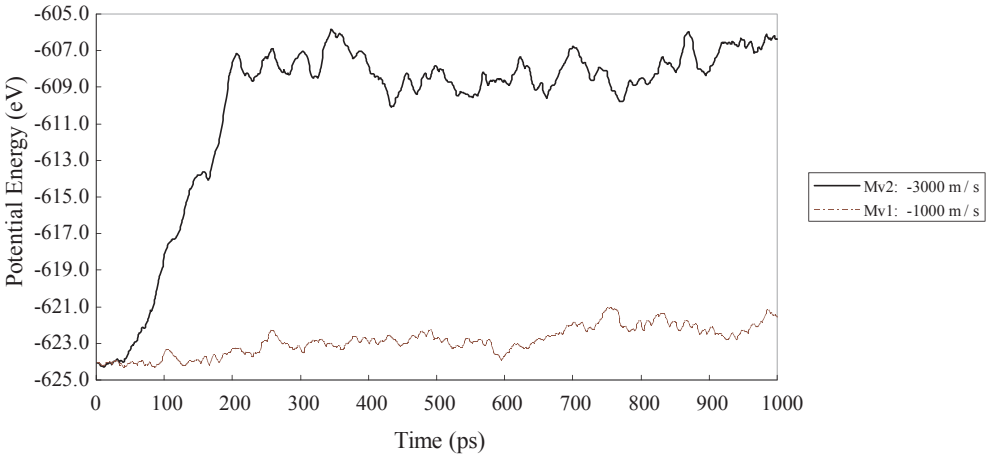

Fig. 5. The BDMNS vertical collision with the Al_3Mg (0 0 1) surface starting at 300 K and two different impact velocities: −1000 m/s and −3000 m/s.

impact speed (kinetic effect) acting on the BDMNS molecule can obviously influence molecular decomposition on surface and surface configuration.

(2). Effect of the substrate temperature: Fig. 7 shows distributions of potential energies for two systems: Mt1 and Mt2, when their BDMNS molecules were colliding vertically towards the Al_3Mg (0 0 1) surface starting at an initial impact velocity $\boldsymbol{V}_z = -1000$ m/s, but beginning at 300 K and 600 K for two slab substrates, respectively. In this Figure, the Mt1 potential curve was identical to that of the Mv1 throughout the whole molecular colliding simulation. However, the Mt2 potential curve represented many sharp peaks throughout the whole colliding simulation. This meant that the BDMNS molecule was obviously dissociating into three pieces once it interacted with the surface: a free Ba ion and two dimethyl-naphthalene-sulfonate rings. And then, these pieces were adsorbing on the surface dynamically, which was similar to those in the Mv2 after 600 time steps. And, the substrate temperature rose to about 860 K from its initial 600 K throughout the whole molecular colliding simulation. In addition, similar to the graphical Fig. 6(b), many more Mg ions were segregating into top layer of the surface from the substrate inside, mainly due to an obvious change of high substrate temperature. From these results, it may conclude that a high substrate temperature (thermal effect) can severely influence molecular decomposition on surface and surface configuration.

(3). Effect of the initial molecular orientation: Fig. 8 shows distributions of potential energies for two systems: Mo1 and Mo2, when their BDMNS molecules were colliding vertically towards the Al_3Mg (0 0 1) surface starting at an initial impact velocity $\boldsymbol{V}_z = -1000$ m/s and beginning at 300 K for two slab substrates, but in two different molecular orientations, respectively. In this Figure, two potential curves performed similarly with less divergence of each other throughout the whole molecular colliding simulation. This may conclude that the initial molecular orientations (geometries) would influence less to the

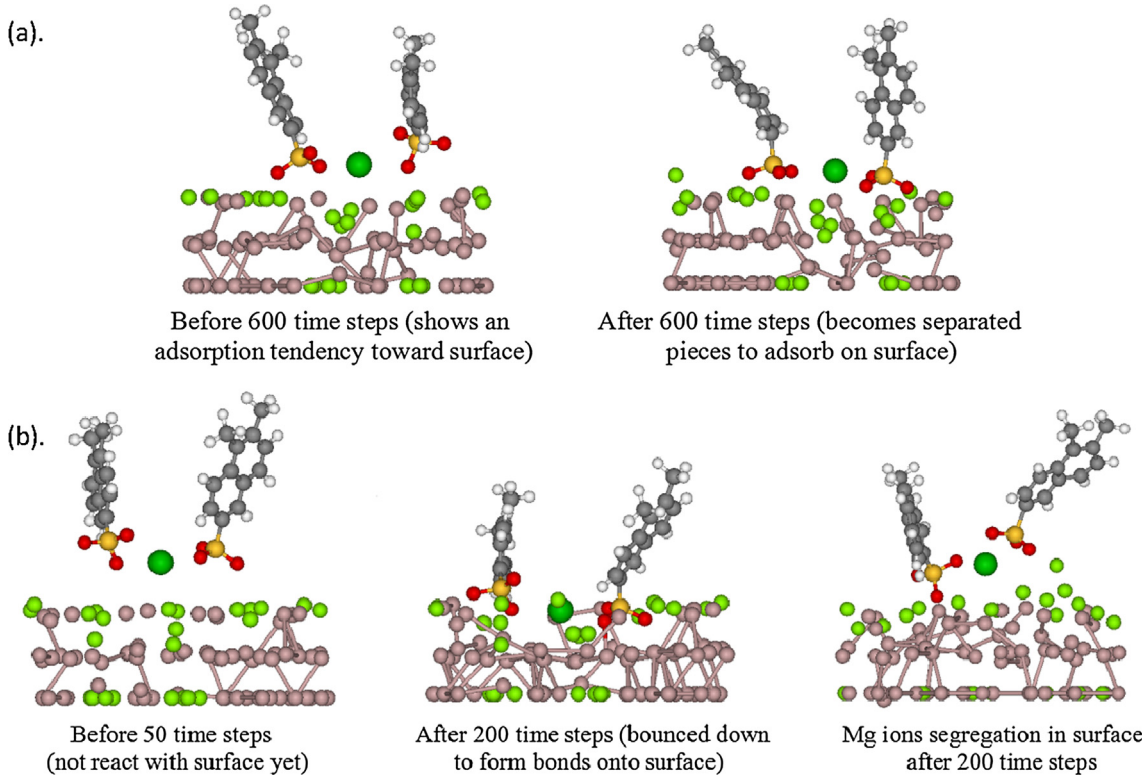

Fig. 6. A BDMNS collision with the Al_3Mg (0 0 1) surface at two systems: (a). Mv1 at $\boldsymbol{V}_z = -1000$ m/s; (b). Mv2 at $\boldsymbol{V}_z = -3000$ m/s.

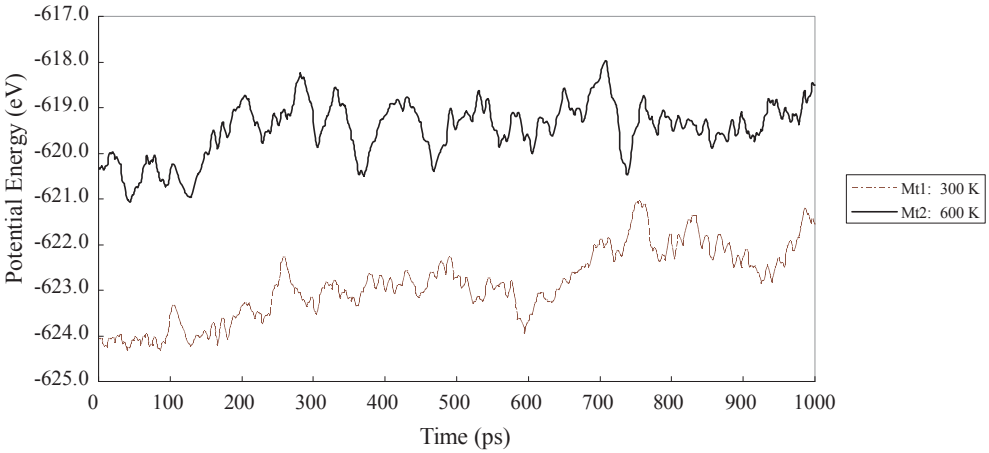

Fig. 7. The BDMNS vertical collision with the Al_3Mg (0 0 1) surface starting at $V_z = -1000$ m/s and two different substrate temperatures: 300 K and 600 K.

BDMNS decomposition on surface.

(4). Beside above simulations, an ancillary work was also carried out: an initial molecular orientation was set up by rotating its two main carbon backbones (rings) 180° relative to the surface plane, with methyl ends (H ions) pointing toward the surface. Simulation result indicated that the whole molecule would bounce off the surface without decomposing. The metal surface plane, even if momentarily became distorted during the molecular impact, it finally relaxed back to a near planar configuration. By the end of the simulation, the BDMNS molecule had rotated its functional groups (S ~ O-bases) back pointing toward the surface, precluding any further interaction.

4.2. Effect of thermal annealing

After all of the colliding simulations in above, an AIMD annealing constraint was then applied to all of above systems under a 300 K environment, so as to make clear whether the decomposed molecular pieces could cover onto surfaces steadily or not. For example, Fig. 9 shows distributions of potential energies for two systems: Mv1 and Mv2, throughout the whole AIMD annealing constraint at 300 K after their colliding simulations as shown in Fig. 5. In this Figure, before 600 time steps, two potential curves were both decreasing to approach their ultimately asymptotic values. After 600 time steps, both of them were running to horizontal levels. This meant that, throughout the whole AIMD annealing constraint, being decomposed, two residual dimethylnaphthalene-sulfonate rings could be adsorbing on the surface steadily by means of their S ~ O bases, plus an adsorption of a free Ba ion on the surface. Such results may corroborate what someone did in refs. [9–10,27]. In addition, many more Mg ions remained segregating into top layer of the surface from the substrate inside, which was very similar to that in graphical Fig. 6 but in less disordered configurations.

4.3. Comprehensive analysis

Factorial design was widely applied to analyses in many experiments and simulations involving several factors, in which it investigated the joint effect of factors on a response. In this Section, a 2^k-factorial design with k factors each at two levels [29], was adopted in analyzing the effect of those variables: the initial impact speed (A), the substrate temperature (B), the initial molecular orientation (C) and their interactions on a response: the binding energy (E_b) between adsorbate and adsorbent calculated by means of a method in Ref. [17]. That was, to better understand the adsorption strength between adsorbate and adsorbent, the binding energy (E_b) was defined as the difference between a total energy of one system combing adsorbate with substrate together, and a sum energy coming from two separated systems with respective adsorbate and substrate, which was expressed as

$$E_b = E(\text{adsorbate \& adsorbent}) - [E(\text{adsorbate}) + E(\text{adsorbent})]. \quad (2)$$

Please note, each system for the E_b calculation in Eq. (2) must be corresponding to its own thermal equilibrium state. By using Eq. (2), a positive E_b value would represent an unfavorable reaction on the surface (a likely decomposition case), while a negative E_b value may

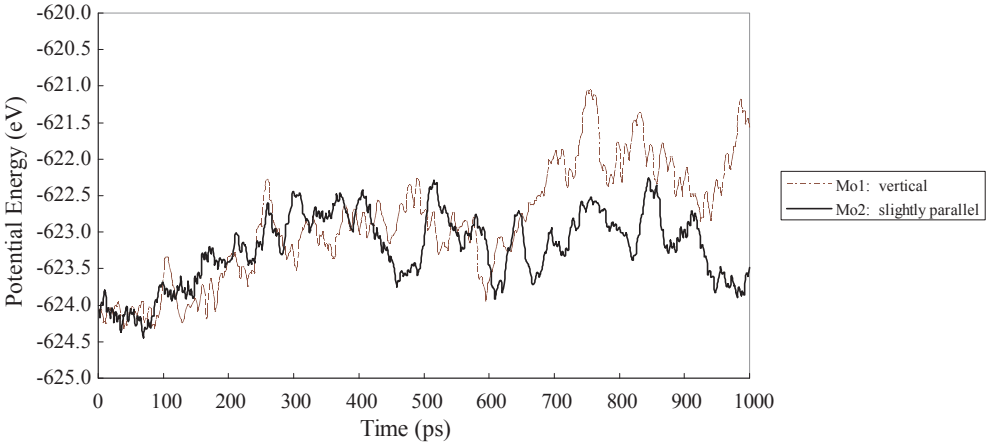

Fig. 8. The BDMNS collision with the Al_3Mg (0 0 1) surface starting at $V_z = -1000$ m/s and a substrate temperature = 300 K, but under two different molecular orientations.

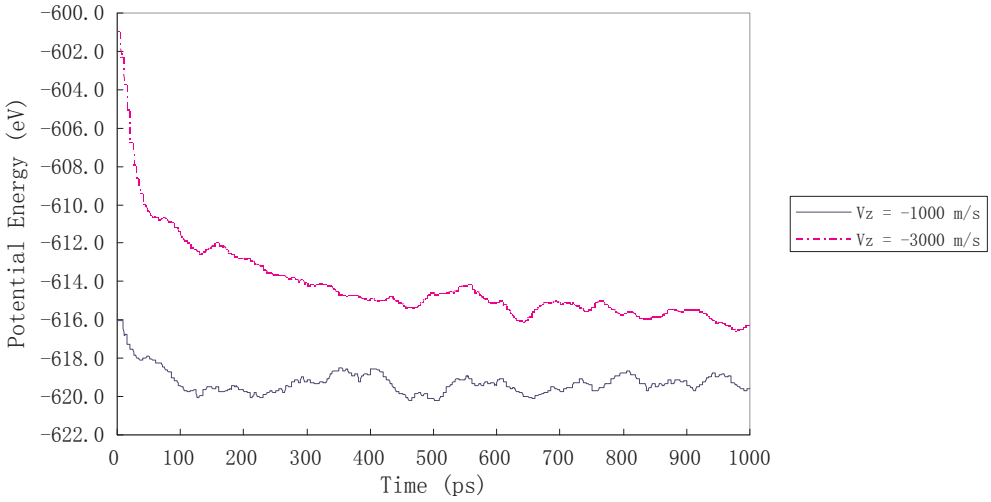

Fig. 9. Potential energies of two systems: Mv1 and Mv2, throughout the whole AIMD annealing at 300 K after their molecular colliding simulations.

represent a favorable reaction on the surface (a likely adsorption case).

Table 3 lists factor contributions to this design. In this Table, two "high (+1)" and "low (−1)" levels were selected for each factor. Thus, $k = 3$ and the total number of combinations was 8. Table 4 shows the response (E_b) for each of 8 simulations (combinations), including the highest (+) and the lowest (−) levels for each factor as shown in Table 3. In this Table, a complete 8 cases (combinations) and a single replicate of E_b (response) were provided for the 2^3-factorial analysis. In this analysis, total 8 runs were made in random order, which corresponded to 8 contrasts (combinations).

Table 5 shows factorial effects for above contrasts and percentage contribution to the response (E_b). From this Table, significant factors emerging from this analysis were main A (10.10%), main B (31.13%), and interactions: BC (11.49%) and AB (8.49%). Therefore, based upon these results, it may conclude that the most significant factor to influence molecular decomposition on surface was the substrate temperature (B), i.e., the higher the substrate temperature (B), the more rapid decomposition of BDMNS on the surface. While the initial impact velocity (A) would play a smaller role. The initial molecular orientation (C) would perform less importance to the decomposition (its negative value just represented a favorable adsorption case). In addition, these results may tell that thermal effect (environmental temperature) would overwhelm kinetic effect (spraying pressure) during the whole molecular decomposition on surface.

Table 4 also told that the response values (E_b) for case 1, 5 and 6 were negative, respectively, implying that these binding states of BDMNS pieces on the surfaces would be favorable (adsorption cases) at very low temperatures, i.e., they would adhere solidly on surfaces at very low temperatures no matter how other factors (e.g., A and C) would perform during the work of surface coating. According to this, a reasonable processing manner for surface protection may follow this way: rise the substrate temperature to a very high point → spray anticorrosive liquids onto the substrate surfaces → make corrosion-inhibitors in liquids decomposing more on the substrate surfaces → descend the substrate temperature to a very low point (even round the room temperature), so as to make those dissociated pieces covering on the substrate surfaces more solidly to perform as corrosion- inhibitors. In fact, during the real processing work, if anticorrosive liquids sprayed onto metal surfaces at a very low environment temperature, anticorrosives in liquids can hardly anchor onto clean surfaces in steady geometries [13]. To overcome this difficulty, before the spraying work, the substrate temperature should increase to a very high value, so that fresh nascent islands in substrate surfaces can be subsequently exposed in the air, which may have anticorrosives more likely react with the surfaces to form solid coverings. Based upon this, people would then spray anticorrosive liquids onto the surfaces. Then next, decreasing the substrate temperature may have those coverings on the surfaces evolve to corrosion- inhibitor thin film in steady geometries. According to this reality, all of our modeling outputs in this article may support the real processing experience.

Table 3
Factor contributions to the 2^k-design.

Factors	Factor levels	
	Low (−)	High (+)
A (initial impact speed)	1000 m/s	3000 m/s
B (substrate temperature)	300 K	600 K
C (molecular orientation)	vertical	parallel

Table 4
The 8 combinations for the 2^3-factorial design.

Case no.	Factor			Response (E_b)
	A (speed)	B (temperature)	C (orientation)	
1	−1	−1	−1	−2.1758
2	+1	−1	−1	1.5336
3	−1	+1	−1	2.5856
4	+1	+1	−1	4.5953
5	−1	−1	+1	−4.0812
6	+1	−1	+1	−3.0684
7	−1	+1	+1	4.2595
8	+1	+1	+1	5.5729

Table 5
Summary of Effect estimate and Percentage contribution.

Model term	Effect estimate	Percentage contribution (%)
A	1.0057	10.095
B	3.1007	31.127
C	−0.4820	4.838
AB	0.8454	8.487
BC	1.1449	11.493
AC	−0.4241	4.257
ABC	0.2500	2.510

5. Conclusions

Ab-initio molecular dynamics based upon density functional theory

was employed to explore a dynamic decomposition pathway for a single barium dimethyl- naphthalene-sulfonate (BDMNS) molecule on a clean Al_3Mg (0 0 1) surface under a high impact condition. Some simulation results were summarized as follows.

At elevated substrate temperatures: 300–600 K, during the AIMD colliding simulations, two residual dimethyl-naphthalene-sulfonate rings on the BDMNS would dissociate from the whole molecule to react with the Al_3Mg (0 0 1) surface via their sulfonic-oxygen bases, plus adsorption of a free Ba ion on the surface. In addition, many more Mg ions were segregating into top layer of the surface from the substrate inside, mainly because of a severe change of high substrate temperature. Finally, throughout the AIMD annealing constraint, molecular pieces would evolve to more favorable coverings on the surface. Besides, an ancillary simulation was running: an initial molecular orientation (geometry) was explored in which the BDMNS was rotated through 180° relative to the surface plane. This simulation may lead the whole molecule to bouncing off the surface without decomposing. Finally, this BDMNS molecule had rotated its "oxygen-rich" functional groups (S ~ O-bases) back pointing toward the surface, precluding any further interaction.

The design-of-experiment (DOE) analysis was applied to these simulations. Three important factors: the initial impact speed acting on molecule (kinetic effect), the substrate temperature (thermal effect), and the initial molecular orientation (spraying angle), were involved in the simulations. The binding energies (E_b) between adsorbates and adsorbents during the whole AIMD annealing constraint were calculated to perform as the response. Results of the DOE analysis indicated that the most significant factor to influence the E_b was the substrate temperature, i.e., the higher the substrate temperature, the more rapid decomposition of BDMNS molecule on the surface. While the initial impact velocity would play a smaller role, and the initial molecular orientation would perform less importance to molecular decomposition. This may also tell that, during the real processing work, thermal effect (temperature) in substrate environment would overwhelm kinetic effect (spraying pressure) to promote molecular decomposition on surfaces. On the other hand, this conclusion implied that, when the substrate temperature descended to a very low point after molecular decomposition on surfaces, those decomposed pieces may bond to surfaces steadily no matter how other factors behaved, which may help optimize the processing way on surface protection.

Acknowledgments

This work was mainly sponsored by the Hebei Provincial Department of Science and Technology Support Program (Grant No.: 15961006D) in China and the National Science Foundation (Grant No.: DMR 9619353) in U.S.A., and supplementarily by the Doctoral Start-up Fund of North China Institute of Aerospace Engineering (Grant No.: BKY-201405) in China. Authors would like to thank Prof. James B. Adams at Arizona State University in U.S.A. for his very valuable comments on this manuscript.

References

[1] P. Wang, B. Yu, H. Li, Drill. Flu. Compl. Flu. 32 (2015) 29–33.
[2] L. Li, J. Qiu, X. Xu, Adv. Fine Petrochem. 16 (2015) 51–53.
[3] Q. Deng, J. Xu, X. Gu, Chem. Res. Appl. 23 (2011) 1324–1327.
[4] Q. Wang, F. Liu, S. Yu, Spec. Petrochem. 25 (2008) 21–24.
[5] X. Yang, Z. Yang, in: Nanjing Int'l. Conf. Ind. Surf. Dvpt., 2007, pp. 29.
[6] X. Yu, H. Zhang, C. Zhang, H. Deng, J. Capital Norm. Univ. 27 (2006) 20–22.
[7] Y. Xu, Y. Tian, Y. Chen, Shandong Chem. Indus. 31 (2002) 7–9.
[8] J. Zhong, H. Wang, J. Li, J. N. China Inst. Aero. Eng. 27 (2017) 1–5.
[9] J.E. Crowell, J.G. Chen, J.T. Yates Jr., J. Electron. Spectrosc. Relat. Phenom. 39 (1986) 97–106.
[10] J.G. Chen, J.E. Crowell, J.T. Yates Jr., Surf. Sci. 172 (1986) 733–753.
[11] J.G. Chen, J.E. Crowell, J.T. Yates Jr., Phys. Rev. B 33 (1986) 1436–1439.
[12] P. Basu, J.G. Chen, L. Ng, J.T. Yates Jr., J. Chem. Phys. 89 (1988) 2406–2411.
[13] R. Underhill, R.S. Timsit, J. Vac. Sci. & Tech. A 10 (1992) 2767–2774.
[14] Y. Jiang, J.B. Adams, Surf. Sci. 529 (2003) 428–442.
[15] Y. Jiang, J.B. Adams, D. Sun, J. Phys. Chem. B 108 (2004) 12851–12857.
[16] L.G. Hector Jr., D.J. Siegel, H. Yu, J.B. Adams, Surf. Sci. 494 (2001) 1–20.
[17] J. Zhong, J.B. Adams, J. Phys. Chem. C 111 (2007) 7366–7375.
[18] Z. Zhang, E.S. Yamaguchi, M. Kasrai, G.M. Bancroft, Tribol. Lett. 19 (2005) 211–220.
[19] M.A. Nicholls, P.R. Nortona, G.M. Bancroft, Y.-T. Cheng, T. Perry, Tribol. Lett. 15 (2003) 241–248.
[20] N.J. Mosey, M.H. Müser, T.K. Woo, Science 307 (2005) 1612–1615.
[21] N.J. Mosey, T.K. Woo, M. Kasrai, P.R. Norton, Tribol. Lett. 24 (2006) 105–114.
[22] G. Kresse, J. Hafner, Phys. Rev. B. 48 (1993) 13115–13118.
[23] G. Kresse, J. Hafner, Phys. Rev. B. 54 (1996) 11169–11186.
[24] D.W. Heermann, Computational Simulation Method in Theoretical Physics, Springer-Verlag, Berlin, 1990.
[25] H.J. Monkhorst, J.D. Pack, Phys. Rev. B 13 (1976) 5188–5192.
[26] J.L. Murray, J. Phase Equili. 3 (1982) 60–73.
[27] J. Zhong, L.G. Hector Jr., J.B. Adams, Phys. Rev. B 79 125419 (2009) 1–14.
[28] J.L. Derissen, J. Mol. Stru. 7 (1971) 67–80.
[29] D.C. Montgomery, Design and Analysis of Experiments, eighth ed., Wiley, New York, 2013.
[30] L. Pauling, The Nature of the Chemical Bond, Cornell University Press, New York, 1960.
[31] G.E. Caballero, P.B. Balbuena, Mol. Simul. 32 (2006) 297–303.
[32] Z. Duan, J. Zhong, G. Wang, J. Chem. Phys. 133 (2010) 114701 1–10.